

Polymorphism and Structural Mechanism of the Phase Transformation of Phenyl Carbamate (PC)

Sara Wishkerman and Joel Bernstein*^[a]

Abstract: Crystallization experiments with phenyl carbamate as a hydrogen-bond donor with crown ethers have led to the discovery of three unknown polymorphs of phenyl carbamate. In this contribution, we characterize the phenyl carbamate polymorphs by a variety of methods including variable

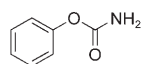
temperature powder X-ray diffraction (PXRD), vibrational spectroscopy (infrared and Raman), calorimetry (DSC)

Keywords: hydrogen bonds · phenyl carbamate · polymorphism · X-ray diffraction

and optical microscopy (HSM). The phase transformation from form I to form II is rapid by both solution-mediated and solid state transformation processes. Through comparison of the two structures of form I and form II it is possible to propose a mechanism for the transformation.

Introduction

As part of a program to develop a strategy for preparation of cocrystals of crown ethers with dihydrogen bond donors with a pre-designed structure,^[1–5] we have carried out experi-



ments to co-crystallize phenyl carbamate (PC) as hydrogen-bond donor with crown ethers. Carbamates, particularly phenyl carbamate derivatives, are known as compounds which ex-

hibit broad pharmacological activities.^[6–9] During co-crystallization experiments of crown ethers with PC we noticed changes in the crystal habits, which prompted additional experiments. These experiments have led to the discovery of three previously unreported polymorphs of pure PC.

In this contribution, we report the results of studies concerning the characterization of these newly discovered PC polymorphs by a variety of methods including variable temperature powder X-ray diffraction (PXRD), vibrational spectroscopy (infrared and Raman), calorimetry (DSC) and optical hot stage microscopy (HSM).

Results and Discussion

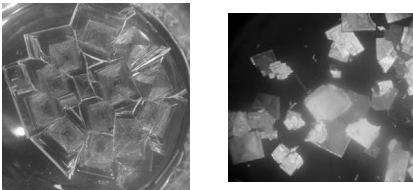
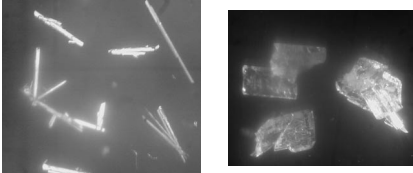
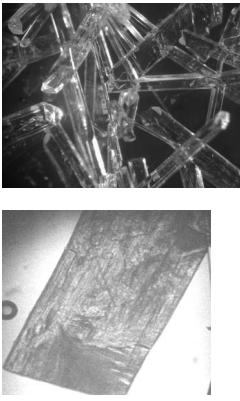
Crystallization: Traditional crystallization experiments were carried out in which saturated solutions of PC were allowed to evaporate from various solvents at slow evaporation rate at room temperature. Crystallization from methanol and acetonitrile produced repeatedly form I in a few days and crystallization from ethyl acetate produced form II in few days. A suspected co-crystal of PC and benzo[18]crown-6 was obtained from solvent-drop grinding experiment^[10] with acetonitrile; the unknown substance is currently under investigation. Form III was observed only on the HSM, PXRD and DSC when a sample of form II was heated. We have not yet succeeded in producing a single crystal of this form. The crystals of different habits are summarized in Table 1.

Form I transforms to form II rapidly in methanolic solution in which the colorless square plates dissolve at the expense of the nearby growing colorless needles and plates. The transformation proceeds until after 120 min the entire sample has converted to the stable form (Figure 1). In other cases the colorless square plates transformed directly and instantaneously into form II (Figure 2).

Thus, form I undergoes both a solution-mediated phase transformation and solid-state transformation to form II.^[11] In addition, form II transforms to form III by heating on the HSM. The phase transformation was observed sequentially as illustrated in Figure 3. The plate shaped form II was heated from 25 to 147 °C. At 80.2 °C form II transforms to form III. It is noteworthy that this observation is not in agreement with the DSC result. The opaque plate of

[a] S. Wishkerman, Prof. J. Bernstein
Department of Chemistry
Ben-Gurion University of the Negev
P.O. Box 653 Beer Sheva, 84105 (Israel)
Fax: (+972) 8-647-7641
E-mail: joel@bgu.ac.il

Table 1. Various crystal habits of PC polymorphs.

Poly-morph	Crystal description	Photograph
form I	colorless square plates	
form II	colorless needles and plates	
form III	white needles and plates	

form III began to melt at 145.1 °C. The transformation processes are summarized in Scheme 1 in accord with the DSC observations.

Diffraction methods of analysis: The crystal structures of form I and form II were determined by single-crystal X-ray diffraction at room temperature. The ORTEP diagram and atomic numbering for both forms are given in Figure 4. Both structures are monoclinic centrosymmetric space group $P2_1/c$ with $Z' = 1$. There are clear differences between the unit cell parameters and the volume which are summarized in Table 2. The calculated density of form II is higher than from I by 4.6%. Thus, the two forms obey Burger's density rule;^[12] that is, the more stable form II has the

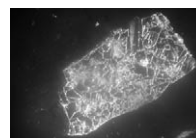


Figure 2. Form II after solid-state phase transformation from form I at room temperature.

higher density. The molecular geometries of the two forms are slightly different in terms of the torsion angle defined by the phenyl ring and the carbamate oxygen. The most significant structural difference between the two molecules in the two forms is the torsion angle C7-O1-C1-C6 which is reduced from 98.4(4)° in form I to 94.0(2)° in form II.

PC has two proton donors and two oxygen acceptor that can participate in hydrogen bond interactions. The hydrogen bonding in the two forms may be compared conveniently with the aid of graph set notation in order to understand the structural similarities and differences of the hydrogen bonding in the system and possibly shed some light on the relative stabilities of the different forms.^[1,13-16] Tables 3 and 4 contain the geometric features and the lengths of the hydrogen bonds. Figure 5 shows the hydrogen bond motifs of the two forms.

Form I is composed of ribbons along the c axis, with alternating $R_2^2(8)$ and $R_{16}^4(16)$, due to the presence of the c glide. In form II there is a translation relationship between molecules along the a axis as shown in Figure 6, leading to a ribbon composed of $R_2^2(8)$ alternating with $R_4^2(8)$. The hydrogen bonds perpendicular to these planes are similar, with the two structures having identical $C(4)$ and $R_2^2(8)$ motifs in the first level graph set. The difference in the ribbon structures is consistent with the greater density of form II.

From the structural analysis of the two polymorphs it is possible to propose a mechanism for the phase transformation. The rapid conversion from form I to form II in the solid state is facilitated by the preservation of the hydrogen-chain packing and the rearrangement of the carbamate group to generate the more dense form. This would roughly involve a flip of the phenyl ring in form I and the formation of an additional $R_2^2(8)$ ring (and consequently the $R_4^2(8)$ ring) with some additional relatively small rotational adjustment of the molecules.

In this context, it is worth mentioning the resemblance of PC and benzamide in their crystal structures and chemical behavior. The disappearing polymorph of benzamide was

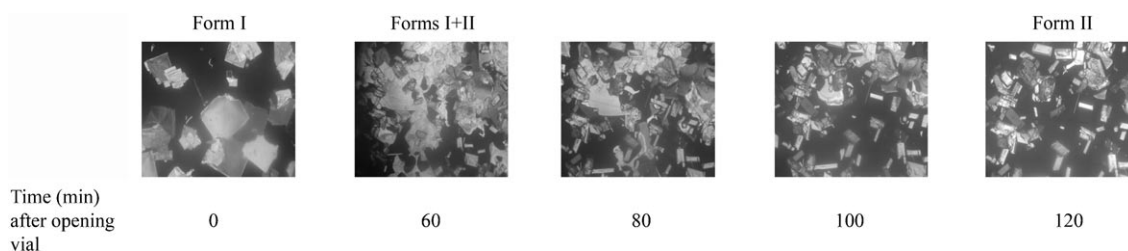


Figure 1. Solution-mediated phase transformation from form I to form II at room temperature.

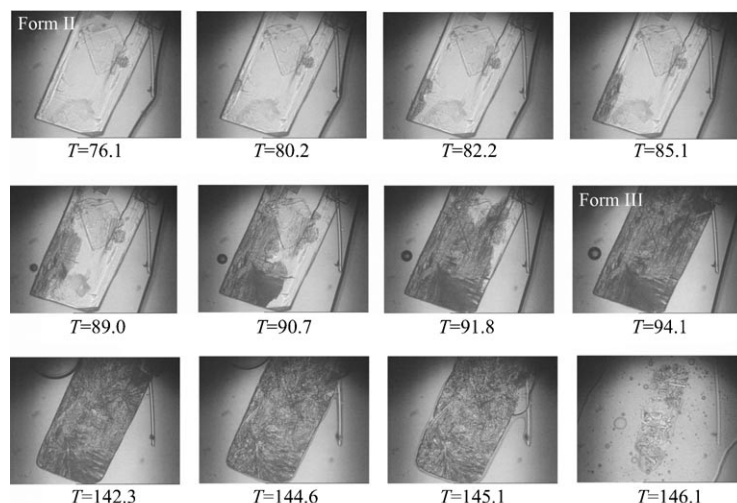


Figure 3. Phase transformation from form II to form III on a Kofler hot stage microscope. The onset of transformation beginning at 80.2 °C in the second photograph is detected by the roughening of the crystal edge. At 145.1 °C form III begins to melt.



Scheme 1. The transformation processes of PC.

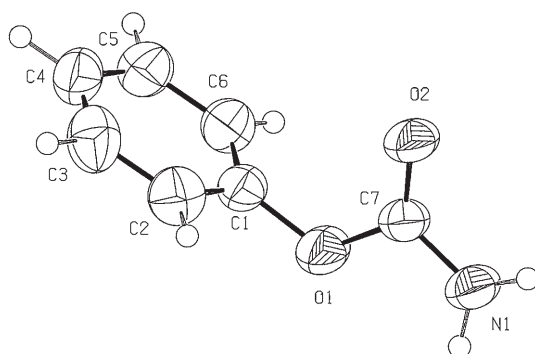


Figure 4. ORTEP diagram and atomic numbering of the molecule in form II. Form I follows the same atomic numbering system.

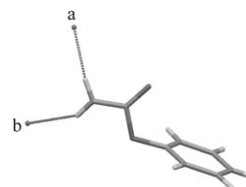
Table 2. Crystallographic data of two PC polymorphs.

	Form I	Form II
crystal system	monoclinic	monoclinic
space group	$P2_1/c$	$P2_1/c$
a [Å]	11.990(2)	5.119(3)
b [Å]	6.352(1)	9.507(5)
c [Å]	9.721(2)	14.436(7)
β [°]	103.01(3)	97.631(9)
V [Å ³]	721(2)	696.2(6)
Z'	1	1
ρ_{calcd} [Mg m ⁻³]	1.263	1.309
R_1 [%]	7.1	4.3

one of the major challenges for chemical crystallographers in the twentieth century.^[17–25] Only recently the crystal structure of the metastable form was solved and the story was

completed.^[26–28] Groth, who summarized the earlier historical work in his 1917 compendium of *Chemical Crystallography*,^[29] described the stable form as a monoclinic prism. The stable forms of both benzamide and PC are monoclinic, $P2_1/c$. The stable form of benzamide also possesses the same ribbon forming $R_4^2(8)$ and $R_2^2(8)$ hydrogen-bond motifs as the stable form of PC. Furthermore the transformation process to the stable form in both compounds occurs via both solid-state phase transformation and solution-mediated phase transformation.

Table 3. Graph set matrices for the hydrogen-bond motifs of PC polymorphs.



Form II	a	b
a	$R_2^2(8)$	–
b	$C_2^1(4)$	$C(4)$
Form II	a	b
a	$R_2^2(8)$	–
b	$R_4^2(8)$	$C(4)$

Table 4. Hydrogen-bond lengths [Å] of PC polymorphs.

	Hydrogen bond a O2–H	Hydrogen bond b O2–H
form I	2.11(3)	2.13(4)
form II	2.12(2)	2.14(2)

The calculated PXRD of form I and form II is shown in Figure 7. Variable temperature PXRD measurements indicate that heating leads to transformation of form II to form III as demonstrated in Figure 8.

IR and Raman spectra: The IR and Raman spectra (Figure 9) provide spectral information corresponding to the nature of the structural differences in hydrogen bonding in the structures.^[30] Major differences between the two polymorphs both at higher and lower wavenumbers in IR spectra and higher wavenumbers in the Raman spectra are due to changes in stretching and deformation vibrations of the phenyl ring. In the spectral regions that are due to hydrogen

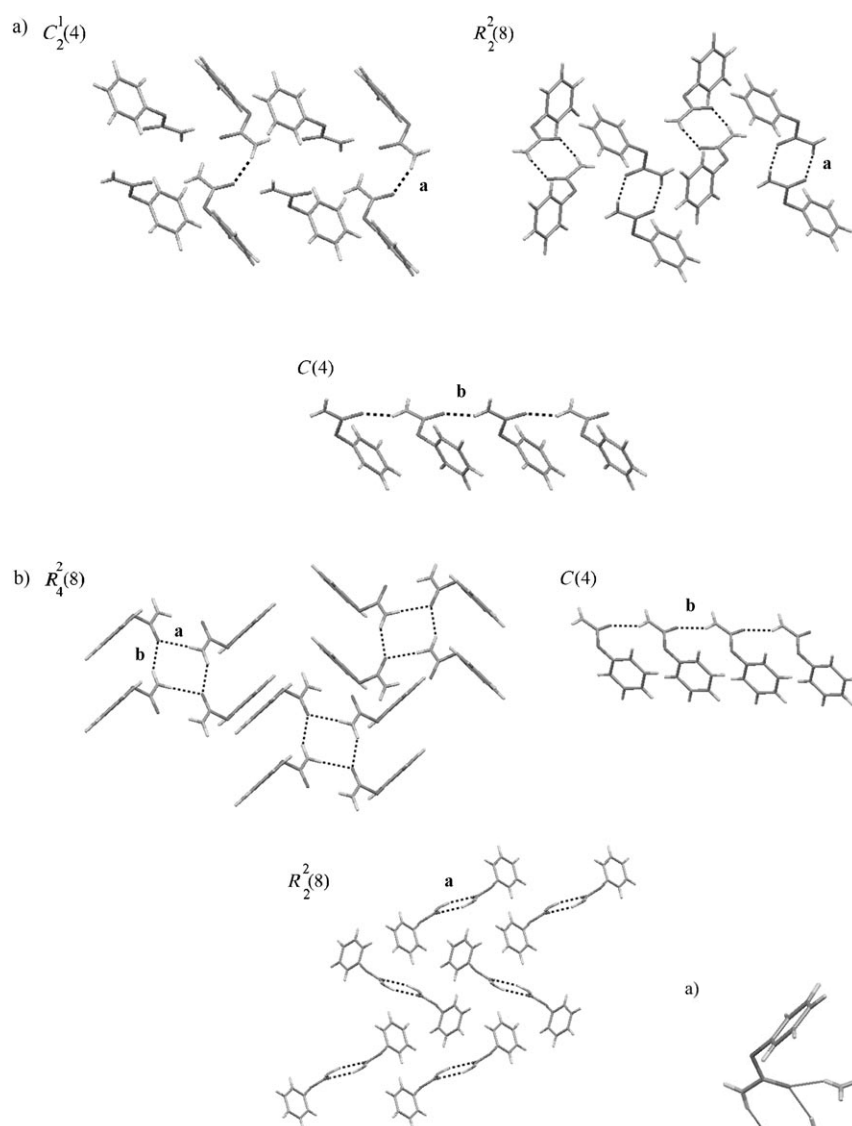


Figure 5. Hydrogen-bond motifs in PC polymorphs a) form I, b) form II. The length of $C(4)$ in form I is 2.13 Å and in form II is 2.14 Å.

bonding minor changes in the stretching vibrations of the amide are observed at higher wavenumbers. The IR peak positions are tabulated in Table 5.

The spectral differences are consistent with observation that a significant difference between the two forms is associated mostly with the environment of the phenyl ring, while the packing diagrams indicate that the hydrogen bonding in both structures appears to be very similar, but the environment of the aromatic ring is indeed different.

Thermal methods of analysis: DSC traces of PC are given in Figure 10. An endotherm of form I melting is observed at 141.7°C (onset) with $\Delta H_f = -3.684 \text{ kcal mol}^{-1}$, and an endotherm of form III melting is observed at 144.4°C (onset) with $\Delta H_f = -5.287 \text{ kcal mol}^{-1}$. The transformation from form II to form III occurs at 95.8°C (onset) with ΔH_t of

$-0.3206 \text{ kcal mol}^{-1}$ (Figure 10). On cooling from the melt of form III, an exothermic peak corresponding to crystallization of form III appears.

The appearance conditions of PC polymorphs and the transformation process emphasizes the balance that exists between kinetic and thermodynamic conditions.^[29] From these results and the crystallization experiments, we can conclude that form I is the kinetically favored form, form II is the stable form at room temperature and form III is the thermodynamically favored form only above 95.8°C.

Conclusions

Co-crystallization experiments of PC with crown ethers have led to the serendipitous discovery of three crystal forms of PC which have been characterized by a variety of techniques. Forms I and II have been ob-

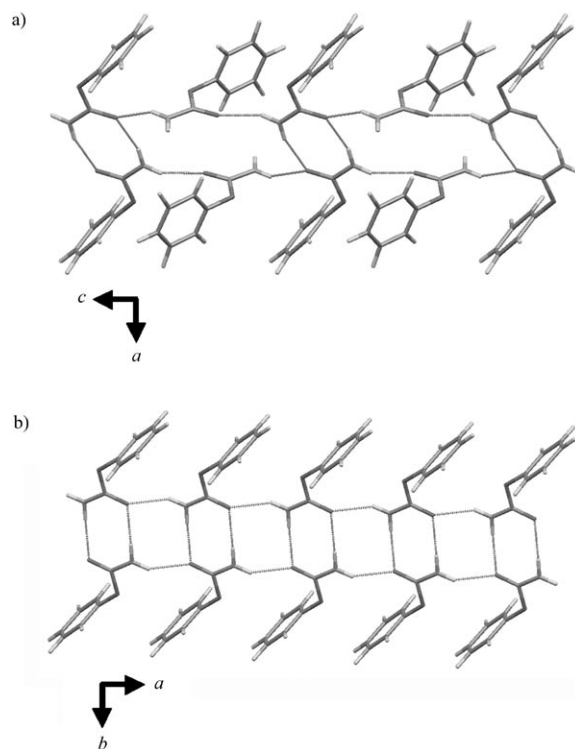


Figure 6. Comparison of the hydrogen chain of a) form I and b) form II of PC.

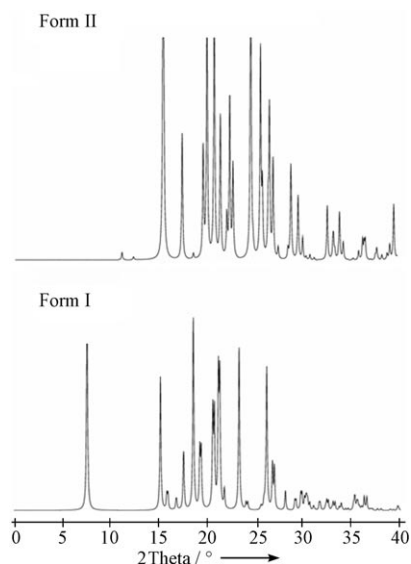


Figure 7. Comparison between the calculated PXRD of form I and form II at room temperature.

tained from a number of solvents while form III was obtained only by heating form II and was observed only transiently in the DSC, HSM and PXRD. Form I transformed to form II both through solution-mediated phase transformation and solid state transformation. A comparison of the two structures of form I and form II provides a qualitative model for the structural mechanism of the transformation. The relatively small changes in IR and Raman peak positions imply that the major differences between the two structures are associated with changes in the environment of the phenyl ring as revealed in the single crystal structure analysis.

Experimental Section

Phenyl carbamate was purchased from Alfa-Aesar and used without further purification.

Laboratory powder X-ray diffraction data were collected on a Huber Guinier Camera 670 which was installed on an Ultrax 18-Rigaku X-ray rotating Cu anode source, with a monochromator (focal length $B=360$ mm) providing pure $K\alpha$ radiation. A position sensitive image plate camera was used for powder diffraction applying transmission geometry. Single crystal X-ray diffraction data were collected on a Bruker SMART 1000 K diffractometer using $MoK\alpha$ radiation with a graphite monochromator. The data were reduced by SAINT,^[31] solved using SHELXS,^[32] and refined with SHELXL^[33] in SHELXTL.^[34] All the atoms (including the hydrogen atoms) were located either in the structure solution or in subsequent difference maps.

Optical microscopy studies were carried out on a Wagner and Munz Kofler Hot Stage mounted on a Leica Galen III model microscope with crossed polarized light.

IR measurements were performed using a Nicolet Impact 410 spectrometer using a KBr disk.

Differential Scanning Calorimetry was carried out on Mettler Toledo Star system. All measurements were run with heating and cooling rate of $5^\circ C min^{-1}$ in sealed Al pans.

Raman measurements were performed by placing the samples under a microscope (Olympus, BX 41) interfaced to a confocal Raman spectrometer (Jobin Yvon, Labram UV HR), driven by the Labspec 4.04 software. Raman scattering was obtained following ≈ 10 mW diode laser excitation at 784.79 nm. The dispersive spectrometer was equipped with a 600 lines mm^{-1} grating and combined with an air cooled charged coupled device (CCD), containing 1024×256 pixels, for Raman signal detection. A TV camera facilitated scanning the sample surface focusing the laser beam on the point to be measured. Spectra were monitored by focusing the laser beam manually or by employing a scannable x,y stage on particular points in the sample. The focusing was done by a X100/0.9 or a X50/0.75 microscope objective to about a $1 \mu m$ spot diameter. A confocal pinhole of $100 \mu m$ diameter, before the entrance slit to the spectrograph, rejected fluorescence and Raman signals from out of focus planes. The spectra were collected over 120 sec and accumulated twice from several points in each sample.

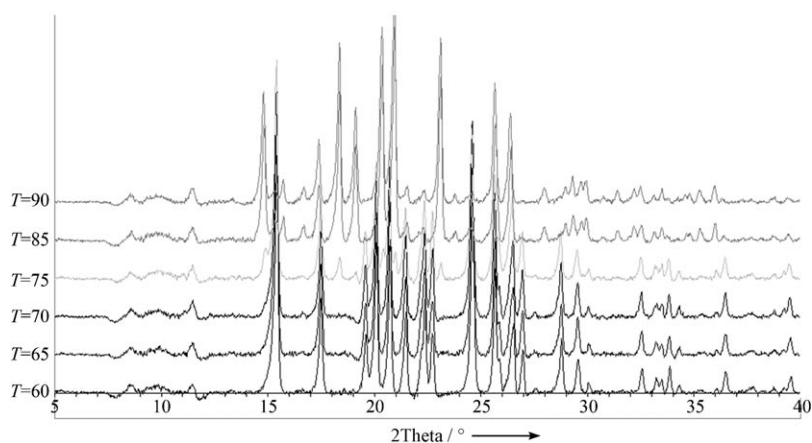


Figure 8. Variable temperature PXRD measurements for the transformation process of form II to form III. The black regions represent form II, the pale gray region represents a transition state during the transformation (i.e., exhibiting both form II and form III) and the dark gray regions represent form III with residue of form II.

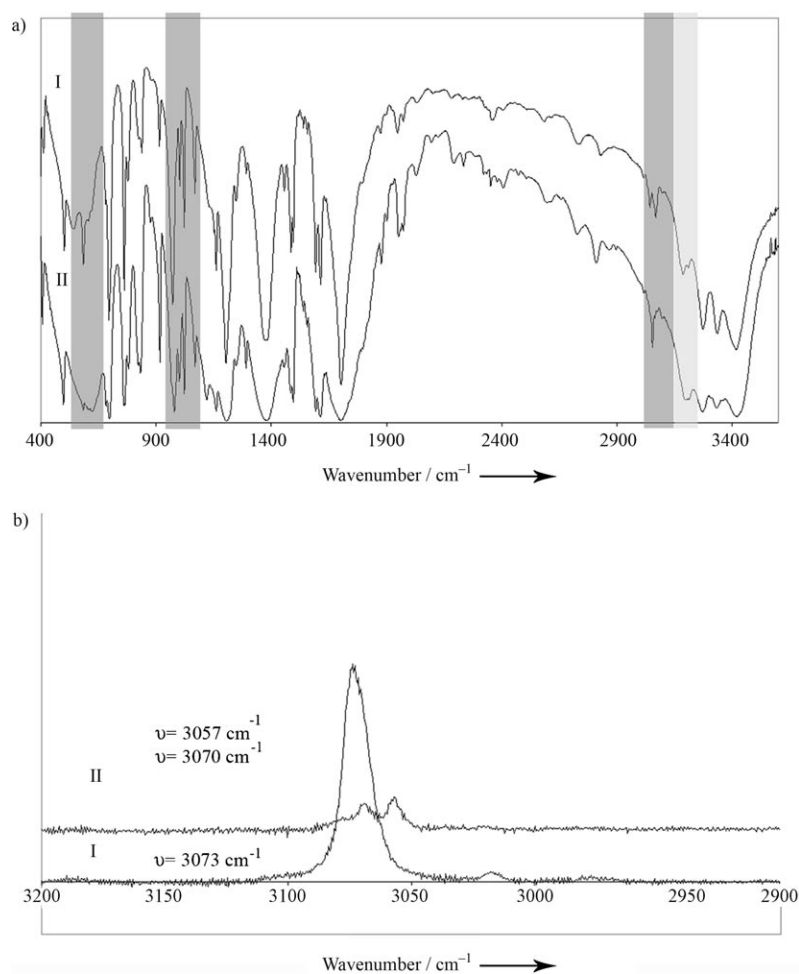


Figure 9. IR spectra of PC I) form I and II) form II: a) the dark gray shaded regions mark the different frequency of the phenyl ring vibrations in the two forms and the pale gray shaded region represent the different vibrations of the amide group. b) 2900–3200 cm^{-1} range of the Raman spectra of PC, showing the changes in stretching vibrations of the amide between the two forms.

Table 5. Summary of IR peak positions of the for the two PC polymorphs.

Frequency [cm^{-1}]	Assignment	
form I	form II	
3050,	3050	aromatic ring: =C-H stretching vibrations
3070		
974	982	aromatic ring: =C-H in plane deformation vibrations
696	690,	aromatic ring: =C-H out of plane deformation vibrations
	700	
548	–	aromatic ring: deformation vibrations
3190,	3220	primary amide: N-H stretching vibrations
3210		

Acknowledgements

We would like to thank Dr. Dimitry Mogilansky for assistance with the powder diffraction measurements in Beer Sheva and to Prof. Ilana Bar for the Raman data. This work was supported in part by a grant from the U.S.–Israel Binational Science Foundation (BSF) Jerusalem, Israel under grant number 2004118.

- [1] J. Bernstein, R. E. Davis, L. Shimoni, N.-L. Chang, *Angew. Chem.* **1995**, *107*, 1687–1706; *Angew. Chem. Int. Ed. Engl.* **1995**, *34*, 1555–1573.
- [2] M. C. Etter, *Acc. Chem. Res.* **1990**, *23*, 120–126.
- [3] Ö. Almarsson, M. J. Zaworotko, *Chem. Commun.* **2004**, 1889–1896.
- [4] S. Datta, D. J. W. Grant, *Nat. Rev. Drug Discovery* **2004**, *3*, 42–57.
- [5] J. J. Remenar, S. L. Morissette, M. L. Peterson, B. Moulton, J. M. MacPhee, H. Guzman, Ö. Almarsson, *J. Am. Chem. Soc.* **2003**, *125*, 8456–8457.
- [6] R. Naito, M. Takeuchi, K. Morihira, M. Hayakawa, K. Ikeda, K. Shibamura, Y. Isomura, *Chem. Pharm. Bull.* **1998**, *46*, 1286–1294.
- [7] W. W. Smith, L. F. Sancilio, J. B. Owera-Atepo, R. J. Naylor, L. Lambert, *J. Pharm. Pharmacol.* **1988**, *40*, 301–302.
- [8] B. Akerman, J. Lars, G. Nilsson, H. Sievertsson, R. Dahlbom, *J. Med. Chem.* **1971**, *14*, 710–740.
- [9] F. Gregan, J. Durinda, E. Racanska, J. Zamocka, *Pharmazie* **1993**, *48*, 465–466.
- [10] A. V. Trask, W. D. S. Motherwell, W. Jones, *Chem. Commun.* **2004**, 890–891.
- [11] R. J. Davey, J. Garside, *From Molecules to Crystallisers*, Oxford Chemistry Primer no. 86, Oxford University Press, Oxford, **2000**.
- [12] A. Burger, R. Ramberger, *Mikrochim Acta* **1979**, 259–271.
- [13] J. Bernstein, M. C. Etter, J. C. MacDonald, *J. Chem. Soc. Perkin Trans. 2* **1990**, 695–698.

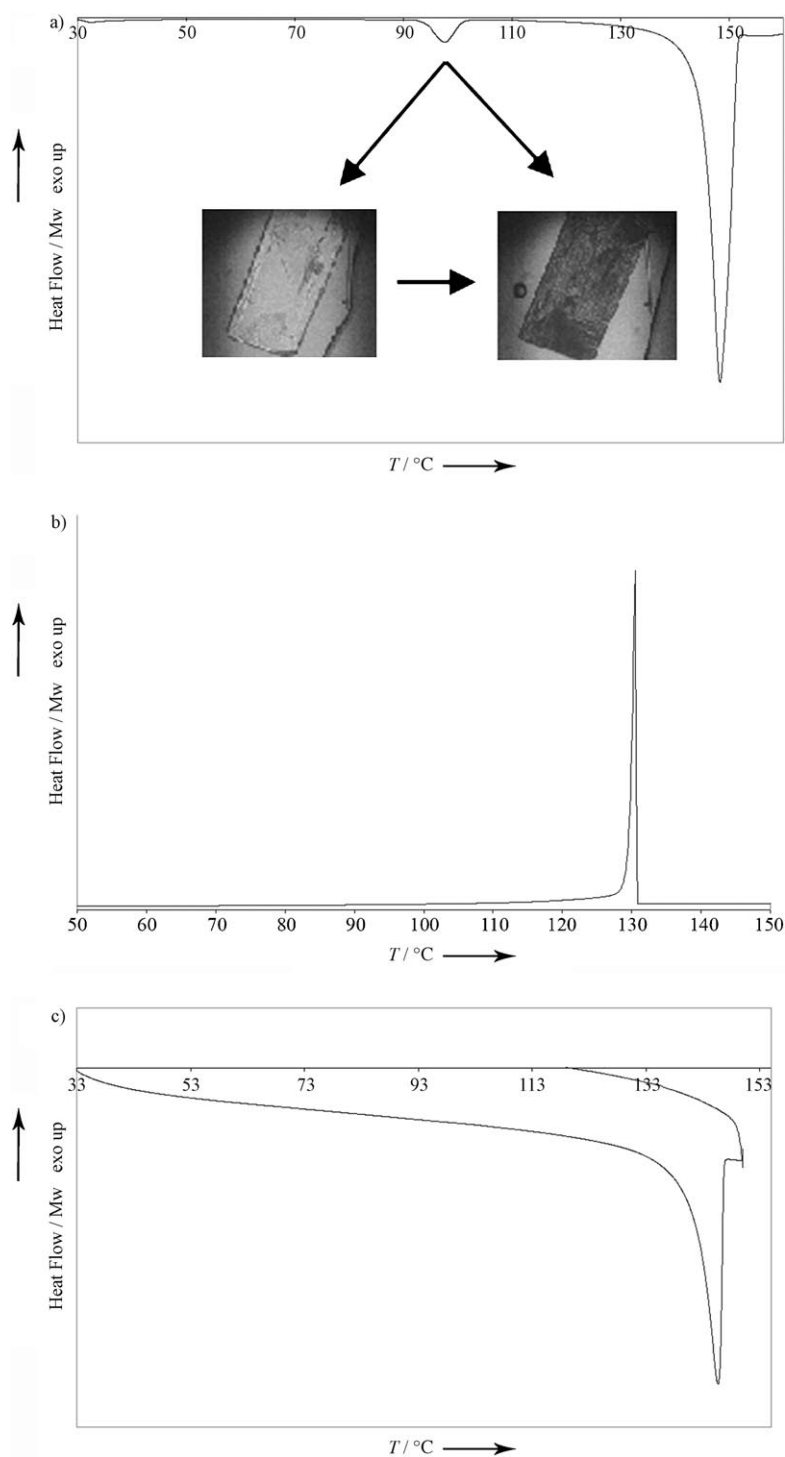


Figure 10. a) DSC thermogram of heating of Form II of PC. b) cooling of form III; c) heating of form I. Both heating and cooling cycle at the rate of $5^{\circ}\text{Cmin}^{-1}$.

[14] M. C. Etter, J. C. MacDonald, J. Bernstein, *Acta Crystallogr. Sect. B* **1990**, *46*, 256–262.

[15] A. F. Wells, *Structural Inorganic Chemistry*, 5th ed., Clarendon, Oxford, **1989**, pp. 294–315.

- [16] W. C. Hamilton, J. A. Ibers, *Hydrogen Bonding in Solids*, Benjamin, New York, **1968**, pp. 19–21.
- [17] W. H. Brock, *Justus von Liebig, the Chemical Gatekeeper*; Cambridge University Press, Cambridge, **1997**.
- [18] *Aus Justus Liebig's und Friedrich Woehler's Briefwechsel in den Jahren 1829–1873, Vol. 1* (Ed.: A. W. Hoffman), Vieweg, Braunschweig, **1888**, pp. 53–54.
- [19] J. von Liebig, F. Woehler, *Ann. Pharm.* **1832**, *3*, 249–282.
- [20] A. Bogojawlensky, *Z. Phys. Chem.* **1898**, *27*, 585–600.
- [21] A. H. R. Mueller, *Z. Phys. Chem.* **1914**, *86*, 177–242.
- [22] E. Mohr, *J. Prakt. Chem.* **1904**, *70*, 307–312.
- [23] B. R. Penfold, J. C. B. White, *Acta Crystallogr.* **1959**, *12*, 130–135.
- [24] C. C. F. Blake, R. W. H. Small, *Acta Crystallogr. Sect. B* **1972**, *28*, 2201–2206.
- [25] J. Bernstein, R. J. Davey, J.-O. Henck, *Angew. Chem.* **1999**, *111*, 3646–3669; *Angew. Chem. Int. Ed.* **1999**, *38*, 3440–3461.
- [26] R. J. Davey, W. Liu, M. J. Quayle, G. J. T. Tiddy, *Cryst. Growth Des.* **2002**, *2*, 269–272.
- [27] N. Blagden, R. Davey, G. Dent, M. Song, W. I. F. David, C. R. Pulham, K. Shankland, *Cryst. Growth Des.* **2005**, *5*, 2218–2224.
- [28] W. I. F. David, K. Shankland, C. R. Pulham, N. Blagden, R. J. Davey, M. Song, *Angew. Chem.* **2005**, *117*, 7194–7197; *Angew. Chem. Int. Ed.* **2005**, *44*, 7032–7035.
- [29] P. Groth, *Chemisches Kristallographie, Vol. IV*, Englemann, Leipzig, **1917**, p. 517.
- [30] G. Socrates, *Infrared and Raman Characteristic Frequencies Table and Charts*, Wiley, New York, **2001**.
- [31] Bruker AXS: SAINT+, Release 6.22. Bruker Analytical System, Madison, Wisconsin, USA, **1997–2001**.
- [32] G. M. Sheldrick, SHELXS-97, Program for the Solution of Crystal Structure, University of Göttingen (Germany), **1997**.
- [33] G. M. Sheldrick, T. R. Schneider, SHELXL-97. Program for the Refinement of Crystal Structure, University of Göttingen (Germany), **1997**.
- [34] G. M. Sheldrick, SHELXTL-Plus, Release 6.10, Bruker Analytical System, Madison, Wisconsin (USA), **2000**.

Received: March 26, 2007

Published online: October 10, 2007